



HAL
open science

Discomfort Glare from a Cyclic Source in Outdoor Lighting Conditions

Joffrey Girard, Céline Villa, Roland Brémond

► **To cite this version:**

Joffrey Girard, Céline Villa, Roland Brémond. Discomfort Glare from a Cyclic Source in Outdoor Lighting Conditions. LEUKOS, 2021, 18 (4), pp.459-474. 10.1080/15502724.2021.1954531 . hal-04444346

HAL Id: hal-04444346

<https://hal.science/hal-04444346>

Submitted on 12 Feb 2024

HAL is a multi-disciplinary open access archive for the deposit and dissemination of scientific research documents, whether they are published or not. The documents may come from teaching and research institutions in France or abroad, or from public or private research centers.

L'archive ouverte pluridisciplinaire **HAL**, est destinée au dépôt et à la diffusion de documents scientifiques de niveau recherche, publiés ou non, émanant des établissements d'enseignement et de recherche français ou étrangers, des laboratoires publics ou privés.

Discomfort glare from a cyclic source in outdoor lighting conditions

Girard Joffrey^{*,1}, Villa Céline^{†,2}, and Brémond Roland^{‡,2}

¹Cerema, AAn, BEE, Les Ponts-de-Cé, France

²Université Gustave Eiffel, CoSys, PICS-L, Champs-sur-Marne, France

Abstract. *Many models of discomfort glare have been proposed for outdoor lighting applications. Most of them were built from data collected in the laboratory in static situations, with motionless light sources, which main characteristics (luminance, size and position) were constant over time. However, on the road at night, drivers are moving with multiple sources around them. To fill the gap between static situations and more realistic ones, four psychophysical experiments were carried out in a laboratory to investigate the impact of the cyclic variations of several light source characteristics (its luminance, eccentricity and solid angle) on the discomfort glare. The temporal frequencies have been chosen representative of outdoor lighting conditions, up to 2.6 Hz. No impact of the dynamics of the glare source was found, except for a source with variable luminance at a low frequency ($f = 0.65$ Hz).*

Keywords: Discomfort glare; LED; Psychophysics; Road lighting; Automotive lighting.

*email adress: joffrey.girard@cerema.fr

†email adress: celine.villa@univ-eiffel.fr

‡email adress: roland.bremond@univ-eiffel.fr

1 Introduction

1.1 Context

The number of LEDs used in outdoor lighting is increasing worldwide, with a market projected to reach USD 21.95 Billion by 2023, and a compound annual growth rate of 12.6% between 2017 and 2025¹. This technology provides important benefits, such as a better light efficiency, and a longer lifetime, but can generate glare, leading to discomfort for road users (Lin et al., 2014; van Bommel, 2015; ANSES, 2019).

Discomfort glare is described by the CIE as “the glare that causes discomfort without necessarily impacting the vision of objects” (CIE, 2013). On the road, it appears when there is too much contrast between the source luminance (headlamps, public lighting) and the background luminance (which is usually associated to the road surface luminance). To predict the discomfort from glare in public and automotive lighting, many models have been proposed in the literature (Hopkinson, 1940; de Boer and Schreuder, 1967; Schmidt-Clausen and Bindels, 1974; CIE, 1976; Bullough and Sweater-Hickcox, 2012; Lin et al., 2014, 2015). Some of them are used in standards, but to date, the issue is still an open question and the recent technical report CIE-243 (CIE, 2021) promotes new research towards a generic model, valid for all applications.

In outdoor lighting, most models predict the mean level of discomfort from glare with respect to the background luminance L_b (in cd/m^2 or fL) and to three factors characterizing the source (labeled here as “main factors”): its luminance L_S (in cd/m^2 or fL), its solid angle ω_S (in steradian) and its eccentricity θ_S (in degree) in the observer’s field of view². Most of these models have been established in static conditions, i.e. when the observer and the light sources are motionless and the sources’ main factors are constant over time. However, at night, road users see glaring lights (luminaires and/or headlamps) scrolling. Therefore, dynamic situations should also be considered, i.e. where the observer is in relative motion with respect to the light sources and the sources’ main factors are varying over time.

¹<https://www.marketsandmarkets.com/Market-Reports/outdoor-led-lighting-market-211822268.html>

²In most indoor lighting models, the *Guth position index* is preferred instead of θ_S

1.2 State of the art

To the best of our knowledge, only one model was created from data collected in dynamic situations: the Glare Control Mark (GCM) (CIE, 1976), derived from the work of de Boer and Schreuder (1967). In their study, the authors asked participants to look inside a box where a mock-up of a road with a lighting installation was presented (scale 1:50). The sources moved toward the participant thanks to a treadmill with an equivalent travel speed of 50 km/h. This experimental device was able to simulate moving conditions at night with a relative motion of the luminaires with respect to the driver. Unfortunately, de Boer and Schreuder (1967) only tested one speed value, and consequently the speed was not considered as a factor in their study, and therefore in the GCM model.

After this pioneering work, some authors have investigated the impact of the source relative speed on the discomfort from glare. Two classes of discomfort from dynamic glare situations have been considered:

- transient glare, when the driver passes a single oncoming car;
- cyclic glare, when the driver meets a series of roadside luminaires or a series of oncoming vehicles, with a periodic visual signal.

1.2.1 Discomfort from transient glare

Sivak and Olson (1988) proposed a methodology to assess the discomfort from glare caused by car headlamps briefly switched on. Participants were asked to drive on a straight road at constant speed (50 or 100 km/h). Another car was stopped on the opposite lane; its headlamps were switched on and off when a participant's car arrived at two specific locations. Then, the discomfort was assessed on a nine-point scale: it was found to be slightly higher at 100 km/h, but the difference was not significant.

In an alternative approach, some authors showed that the discomfort depends on the duration of the exposition to glare. Ahmed and Bennett (1978) found, in a lab experiment, that for very short time lapses (below 0.2 s), the observers felt less discomfort than for longer ones. Between 0.5 and 5 s, the discomfort from glare was almost constant, and decreased slowly up to 10 s. Lehnert (2001) found that the discomfort from glare continuously increases

when the time lapse increases from 0.2 to 10 s. Sivak et al. (1997) had similar results with real headlamps with time lapses between 0.125 and 2 s. Despite the differences across studies, it is clear that the time the lamp is on has an effect on the discomfort from glare.

1.2.2 Discomfort from cyclic glare

Irikura et al. (1998) have investigated the effect of the temporal frequency of a flashing light in central vision on the discomfort. They tested flashing frequencies between 1 and 16 Hz, with background luminances between 0.1 and 100 cd/m^2 . The light source was on average less uncomfortable in the static conditions than in the dynamic conditions, whatever its temporal frequency. The discomfort was maximum in the 5-8 Hz range. Focusing on the periodic luminance variation, Irikura's study can also be related to discomfort from visual flicker.

A series of studies were also carried out at the Kansas State University, investigating the impact of a cyclic exposition to glare on discomfort with a specific experimental device: the "Fry simulator" (see Anantha (1982) and Hussain (1985) for a technical description). In two similar studies testing the influence of the source speed on the discomfort from glare (Easwer, 1983; Ganesh, 1986), the participants sat in a kind of cabin car, and the scrolling of street luminaires was simulated with a real lamp in front of them. They rated the discomfort at simulated speeds of 48 km/h and 97 km/h. Simulated motion at 48 km/h produced less discomfort than at 97 km/h; the static condition produced even less discomfort. After some modifications, this simulator was later employed by Liu and Konz (1991), who considered three speeds: 64, 80 and 97 km/h. Unlike Easwer (1983) and Ganesh (1986), they did not find any significant effect of the simulated speed on the discomfort from glare.

In the studies simulating a cyclic glare as on the road, no consensus was reached regarding the impact of the relative speed on discomfort. In these previous experiments, all the main source factors (luminance L_S , eccentricity θ_S and solid angle ω_S) varied together. Thus, one cannot separate the effect of a given factor from the effect of the others. Therefore, in the present study, we will consider the temporal variations of each of these factors in separated

experiments, by keeping the other factors constant, to assess the influence of the variation of each factor on the discomfort from glare.

1.3 Objective of the work

Under an outdoor lighting installation, the sources have a constant spacing: if an observer drives at constant speed along the luminaires, he experiences an apparent cyclic motion of the sources in his visual field. Given that discomfort from glare from several sources is equivalent to a single source producing the same discomfort (Girard et al., 2019), we have focused on the periodic motion of one source. In addition, in a public lighting installation, we know from previous literature that the luminaire closest to the driver provides most of the discomfort (Bennett, 1987; Bullough et al., 2008).

We have studied the impact of temporal variations of the three main source factors on discomfort from glare. Four psychovisual experiments have been carried out independently in a laboratory. Experiment 1 analyzes the impact of the source motion itself on the discomfort, with the main factors (L_S , ω_S and θ_S) remaining constant. Experiments 2, 3 and 4 address respectively the impact of the periodic variations of the source luminance L_S , of its eccentricity θ_S and of its solid angle ω_S on the discomfort, the other factors being constant.

The paper is organized as follows. The experiments are described in Section 2. The results of the four experiments are presented in Section 3, and a discussion is proposed in Section 4.

2 Material and method

2.1 Participants

In all four experiments, the panels included 40 participants.

- In Experiment 1, there were 14 women and 26 men, between 21 and 62 years old ($M=37.8$, $\sigma = 12.7$);
- In Experiment 2, there were 15 women and 25 men, between 20 and 63 years old ($M=36.6$, $\sigma = 12.4$);

- In Experiments 3 and 4, there were 17 women and 23 men, between 21 and 59 years old ($M=34.2$, $\sigma = 11.2$). The panel was the same for these two experiments: they were carried out one after the other, in a random and balanced order.

The majority of the participants were employees of the university. All were initially naive to the purposes of the experiments. Before each experiment, they received instructions and signed an informed consent form. They wore their usual ocular corrections (glasses or lenses) if any. Then, they passed a visual acuity test with an Ergovision device (Essilor) to check that they had a visual acuity above 5/10, which is the visual acuity threshold in the French traffic regulations (DOT, 2005).

2.2 Overview of the experiments

2.2.1 General description of the setups

In the four experiments, participants sat in front of a screen in a dark room (no window and no light source other than those described in the experiment). A lamp was located behind the participant in order to generate a background luminance on the screen surface around 1 cd/m^2 , which is a typically recommended value for street lighting in the European standard (CEN, 2015). The participants were instructed to keep their gaze on a fixed target located 1.59 m in front of them. The use of a head rest ensured that the participant's eyes and the target stayed in the same horizontal plan.

The target was selected from previous studies, where a specific design is emphasized, allowing the best gaze stability (Thaler et al., 2013; Lee et al., 2017). It was visible in mesopic conditions (see Figure 1). The participants fixations were controlled with a SMI deported eye-tracker during Experiments 1, 3 and 4 (this eye-tracker was not available for Experiment 2). It was located on a table in front of the participants and calibrated from nine points: the target and eight red points spread over the screen (see Figure 1).

The four experiments were conducted with specific experimental devices in order to isolate and manipulate each experimental factor independently. These devices are described in sections 2.3 to 2.6.

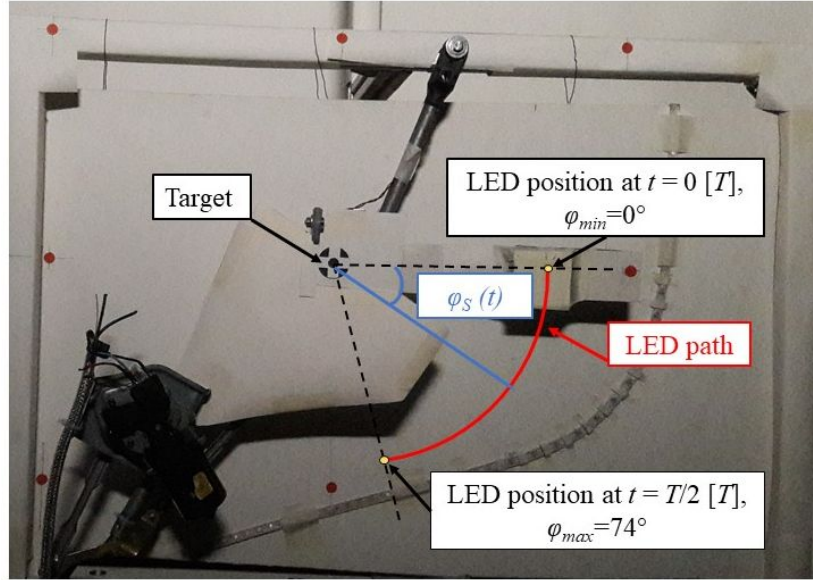


Figure 1: Experimental device in Experiment 1. The LED trajectory is marked in red; the target and the eye-tracker calibration points are also presented.

2.2.2 Experimental conditions

In each experiment, two types of visual conditions were presented to the participants:

- **dynamic conditions**, where one experimental factor y was changing over time. The signal $y(t)$ was periodic, varying between y_{min} and y_{max} with a temporal frequency f and a temporal modulation index m :

$$m = \frac{y_{max} - y_{min}}{y_{max} + y_{min}} \quad (1)$$

- **static conditions**, considered as control conditions with respect to the dynamic conditions. One static condition was common in the four experiments, with $\theta_S = 10^\circ$ and $\omega_S = 5 \times 10^{-6} \text{ sr}$.

To chose the time course of the signal, the range of variations of each factor and the range of temporal frequencies representative of public lighting

for each factor, computer simulations have been conducted. The luminaire closest to the driver was simulated, as it provides most of the discomfort (Bennett, 1987; Bullough et al., 2008). The variation of each of the associated source factors were simulated at various driving speeds, between 30 and 130 km/h. The luminaires height were simulated between 7 and 12 m. Based on professional practice (AFE, 2002), the luminaire spacing was set to $3.5h$ in these simulations. For instance, a vehicle speed between 30 and 130 km/h when $h = 8$ m leads to temporal frequencies of the light source factors between 0.30 and 1.30 Hz. We based our calculations on actual luminaires data.

The case of automotive lighting was also considered (with two cars crossing each other). An “observer vehicle” was simulated, driving at a constant speed and crossing a succession of “oncoming vehicles”, also driving at (another) constant speed. The inter-distance between two consecutive oncoming vehicles was constant, computed from the safety distance of 2 s between two consecutive vehicles (DOT, 2003). The crossover frequency between the observer vehicle and the closest oncoming vehicle was computed as a function of the driving speeds. For instance, an observer vehicle driving at 90 km/h and passing a succession of oncoming vehicles with speeds between 10 and 130 km/h leads to temporal frequencies of the light source factors between 0.80 and 2.91 Hz. For this scenario, our calculations were based on headlamp data provided in the report CIE-188 (CIE, 2010).

Table 1 summarizes the ranges of temporal frequency of the source factors estimated from these simulations, for public and automotive lighting. It also gives the minimal and maximal values of each factor in these simulations, as well as the range of the modulation index. From these scenarios, frequencies between 0.2 and 4 Hz are relevant for discomfort glare on the road. In our experiments however, temporal frequencies are limited between 0.33 and 2.60 Hz, because extreme values only concern rare scenarios.

2.3 Experiment 1: Impact of the motion

2.3.1 Experimental setup

In Experiment 1, a RGB LED glare source was displayed with a cyclic motion, while its mains factors (θ_S , L_S and ω_S) were constant over time. To

Table 1: Simulations of public and automotive lighting. Range values of temporal frequency, eccentricity, solid angle and luminance are given for each situation, with the corresponding modulation index.

| Source Factor | Public Lighting | | Automotive lighting | |
|-------------------------------------|--|--------------|--|-----------|
| | Range value | m | Range value | m |
| Temporal frequency f (Hz) | [0.2; 1.5] | NA | [0.5; 4.0] | NA |
| Eccentricity θ_S (degree) | [8; 20] | 0.40 to 0.42 | [2; 60] | 0.50 to 1 |
| Solid Angle ω_S (sr) | $[2.9 \times 10^{-7}; 3.0 \times 10^{-5}]$ | 0.93 to 0.94 | $[6.2 \times 10^{-7}; 1.4 \times 10^{-4}]$ | 0.90 to 1 |
| Luminance L_S (cd/m^2) | $[2.0 \times 10^4; 1.5 \times 10^5]$ | 0.57 to 0.61 | $[10^3; 10^5]$ | 0.90 to 1 |

meet these constraints, the source followed a circular trajectory in a plane orthogonal to the participant’s line of sight (see Figure 1), then came back to its initial position, and again. The center of rotation was the target and the radius corresponded to the eccentricity θ_S .

According to Kim and Kim (2010), the discomfort glare is nearly constant, at the Borderline between Comfort and Discomfort (BCD) along arcs of constant eccentricity in the lower field of view, for eccentricities below 30° , and for angles lower than 67.5° between the horizontal axis and the position of the source (φ_S in Figure 1). In this range, the BCD iso-luminance curves are circular in shape.

The experimental device was built from a windshield wiper mechanism, allowing a continuous semi-circular motion below the horizontal axis, at constant speed. The wiper arm was fixed on a metallic structure, and was placed in front of the white screen. At the beginning of each trial, the arm was automatically positioned on the horizontal axis. The target was attached to the center of rotation of the wiper’s arm, and the LED was fixed at the arm’s end. The experimental device allowed a periodic motion of the LED, with an angle φ_S between 0° (on the horizontal axis) and 74° below the horizontal axis, which was the functional range of the wiper.

The luminance values of the LED have been calculated from vertical illuminance measurements at the observer’s eyes considering the LED diameter of 4 mm. As the three chips in the RGB LED were smaller than the LED itself, the computation based on illuminance measurements was validated by comparing with the direct measurement of the luminance of one LED. These measurements were conducted with a LMT B520 luxmeter with the photoreceptor cell directed toward the target. To estimate the illuminance from the 8-bit gradation of the LED, seven measurements were made between the minimal and maximal intensities of the source. The relation was found linear with a strong correlation ($R^2 = 0.997$). The range of luminance values available in this experiment is provided in Table 2 (see Exp. 1).

Table 2: Glare source and background luminance range in each experiment. L_{min} and L_{max} are the minimum and maximum luminance values available for the glare sources in each experiment. Each psychophysical staircase began with an initial luminance L_{ini} , and an initial luminance step $L_{step,ini}$. The last two columns provide the background luminance in each experiment (mean luminance and SD, as well as the type of lamp).

| Exp. | Eccentricity (°) | Glare source | | | | Background | |
|------|---------------------|---------------------------|---------------------------|---------------------------|--------------------------------|----------------|---|
| | | L_{min} (cd/m^2) | L_{max} (cd/m^2) | L_{ini} (cd/m^2) | $L_{step,ini}$ (cd/m^2) | Lamp | Mean L_b (σ) (cd/m^2) |
| 1 | 10° | 284 | 64297 | 15987 | 7871 | 5600-K LED | 1.12 (0.55) |
| 2 | 5° | 493 | 25119 | 6403 | 3152 | 3000-K halogen | 0.92 (0.17) |
| | 10° | 484 | 24674 | 6289 | 3096 | 3000-K halogen | 0.92 (0.17) |
| 3 | 5° – 15° | 1237 | 63088 | 16081 | 8659 | 5600-K LED | 1.04 (0.75) |
| 4 | 10° | 1420 | 64463 | 16391 | 8070 | 5600-K LED | 1.04 (0.75) |

The background luminance was provided by a 5600-K LED lamp located behind the participant. The background luminance was measured with a Konica Minolta CA-2000 videophotometer (see Table 2).

2.3.2 Experimental protocol

The protocol of this experiment consisted in collecting luminance data at the Borderline between Comfort and Discomfort (BCD). The BCD is commonly used to assess the discomfort from glare (Luckiesh and Guth, 1949;

Putnam and Gillmore, 1957; Bennett, 1977; Irikura et al., 1998). The BCD threshold was reached using the staircase method (Cornsweet, 1962). This method is broadly used in psychophysics to estimate perception thresholds (including in acoustics, pain, etc.). Bargary et al. (2015) used it to assess the discomfort from glare, but not many other studies in the literature have considered it.

Each experimental condition was implemented with a staircase, allowing to reach the BCD threshold. A staircase was a succession of trials. In each of these trials, the light source was switched on for four seconds, then switched off. If a participant felt discomfort during a trial, he had to decrease the luminance of the source in the next trial by clicking the right button of a mouse. If not, he clicked the left button to increase the luminance in the next trial. At the end of the staircase, the luminance adjusted by the participant was assumed to generate a level of discomfort close to his own BCD.

Each staircase began with the same initial luminance value L_{ini} and the same initial luminance step $L_{step,ini}$ (see Table 2). The luminance step was halved each time the participant changed his judgment with respect to the previous trial³. The luminance step could not be lower than a minimal step value $L_{step,ini}/8$.

For a given staircase, the participants went through a maximum of 16 trials. The BCD luminance was estimated as the mean luminance of the four last trials in the staircase. If the left and right buttons of the mouse were alternated for six consecutive trials, it was considered that the BCD was reached and the staircase was stopped. At the end of a staircase, a sound was emitted, alerting the participant that the next staircase was about to begin.

Participants went through a training session before the experiment, with experimental conditions different from those in the test session. The participants had time to adapt their eyes to 1 cd/m^2 during the instructions and the training session, which lasted about 15 minutes in each experiment. The experiment lasted about 45 minutes.

³For instance, when the participant clicked the right button for trial number i , and then clicked the left button for trial number $i + 1$.

2.3.3 Experimental design

The temporal profile of the source motion periodic signal is provided on Figure 2(a).

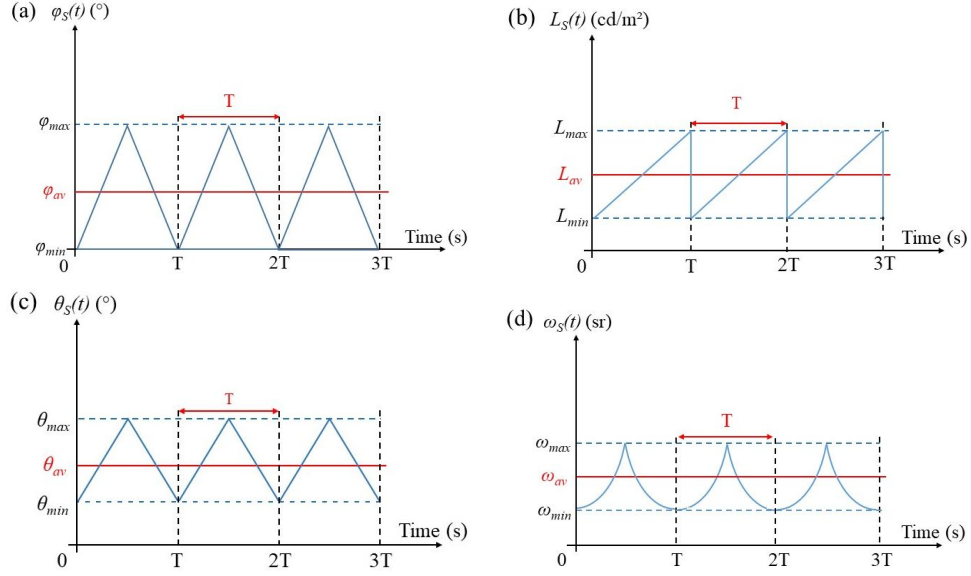


Figure 2: Periodic signals of each source factor variation in the four experiments: (a) Profile of the angle $\varphi_S(t)$ in Experiment 1; (b) Profile of the luminance $L_S(t)$ in Experiment 2; (c) Profile of the eccentricity $\theta_S(t)$ in Experiment 3; (d) Profile of the solid angle $\omega_S(t)$ in Experiment 4.

The experimental design of this experiment is provided in Table 3 (see Exp. 1: Motion), which shows the temporal frequency of each dynamic condition. The modulation index is $m = 1$, meaning that $\varphi_S(t)$ reaches 0° (see Eq. 1).

In this experiment, the temporal frequency of the source motion could not be greater than 1 Hz, due to the technical limits of the motor.

Table 3: Experimental design and values of the source factors in the four experiments.

| Experiment | Condition | Temporal frequency (Hz) | LED eccentricity θ_S (degree) | LED solid angle ω_S (sr) | Temporal modulation index m |
|--------------------------------|-----------|-------------------------|--------------------------------------|---|-------------------------------|
| Exp. 1: Motion | Dynamic | 0.33 | 10° | 5×10^{-6} | 1 |
| | Dynamic | 0.66 | | | |
| | Dynamic | 1.00 | | | |
| | Static | 0 | | | |
| Exp. 2: Luminance variation | Dynamic | 0.65 | 5° | 5×10^{-6} | 0.65 |
| | Dynamic | 1.30 | | | |
| | Dynamic | 2.60 | | | |
| | Static | 0 | | | |
| | Dynamic | 0.65 | | | |
| | Dynamic | 1.30 | | | |
| | Dynamic | 2.60 | | | |
| Static | 0 | | | | |
| Exp. 3: Eccentricity variation | Dynamic | 0.50 | [5°; 15°] | 5×10^{-6} | 0.50 |
| | Dynamic | 1.25 | [5°; 15°] | | |
| | Dynamic | 2.50 | [5°; 15°] | | |
| | Static | 0 | 10° | | |
| Exp. 4: Solid angle variation | Dynamic | 0.50 | 10° | [8.8×10^{-8} ; 1.4×10^{-5}] | 0.99 |
| | Dynamic | 1.25 | | [8.8×10^{-8} ; 1.4×10^{-5}] | |
| | Dynamic | 2.50 | | [8.8×10^{-8} ; 1.4×10^{-5}] | |
| | Static | 0 | | 5×10^{-6} | |

2.4 Experiment 2: Impact of the luminance variations

2.4.1 Experimental setup

A semi-circular structure was placed horizontally at the height of the participant's eyes (see Figure 3), with the center of the circle at the position of the observer's eyes. A RGB LED strip was attached to this structure in such a way that the two LEDs used in the experiment at 5° and 10° eccentricity were seen by the participants at the same distance, and consequently with the same solid angle ($\omega_S = 5 \times 10^{-6} \text{ sr}$).

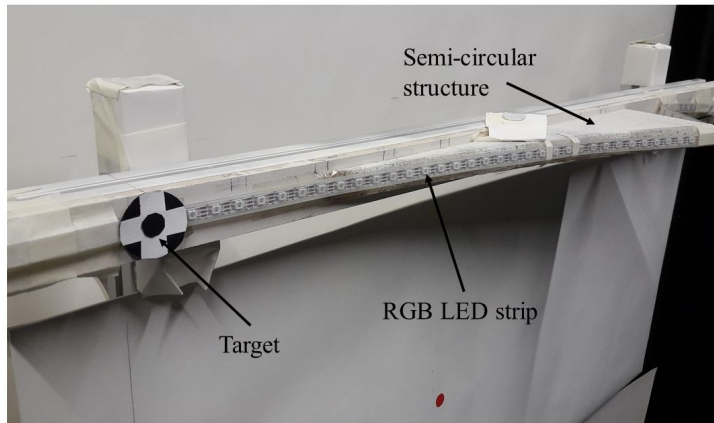


Figure 3: The horizontal LED strip attached to a semi-circular structure, with the target, in Experiments 2 and 3.

The luminance values of the glare sources were calculated from vertical illuminance measurements, with a LMT B520 luxmeter and seven intensity setting values. The relation between the luminance and the intensity setting was found linear ($R^2 > 0.999$). For a given intensity setting, the LEDs were expected to emit the same luminance whatever their eccentricity. Measurements reported in Table 2 (Exp. 2) show that L_{min} and L_{max} are very close for both eccentricities.

A 3000-K halogen lamp was placed behind the participant in order to provide a background luminance of 1 cd/m^2 . It was as uniform as possible on the screen. The mean luminance value and SD have been estimated with a Konica Minolta CA-2000 videophotometer (see Table 2).

2.4.2 Experimental protocol

The experimental protocol was the same as described in Section 2.3.2, except for the values of L_{ini} and $L_{step,ini}$ (see Table 2). During the staircase, it was the time-averaged luminance L_{av} which was increased or decreased according to the participants' choice (see Figure 2(b)). Because of the technical constraints of the device, the range of L_{av} was larger in the static than in the dynamic conditions, due to the difference of the temporal modulation index m of the luminance variations:

- in static conditions, L_{av} could vary between L_{min} and L_{max} (see Table 2);
- in dynamic conditions, L_{av} could vary between $\frac{L_{min}}{1-m}$ and $\frac{L_{max}}{1+m}$, i.e. between 1409 and 15224 cd/m^2 for $\theta_S = 5^\circ$ and between 1383 and 14954 cd/m^2 for $\theta_S = 10^\circ$.

The experiment lasted between 45 minutes and 1 hour.

2.4.3 Experimental design

The temporal profile of the source luminance periodic signal was designed with reference to our simulations (see Figure 2(b)).

The experimental design of this experiment is described in Table 3 (see Exp. 2: Luminance variations). Static and dynamic conditions were presented for two eccentricities (5° and 10°). The purpose was to test for a possible interaction between eccentricity and temporal variation of the source luminance (Waters et al., 1995; Eble-Hankins and Waters, 2004; Stringham and Snodderly, 2004). Moreover, the static condition with $\theta_S = 10^\circ$ was repeated at the end of the experiment, in order to estimate the intra-individual variability. Thus, nine staircases were adjusted during the experiment.

The luminance frequency varied between 0.65 and 2.6 Hz, which is included in the range computed in the simulations (see Section 2.2.2), and corresponds to the lowest part of the range of frequencies producing visual flicker. In all dynamic conditions, the modulation index was $m = 0.65$.

2.5 Experiment 3: Impact of the eccentricity variations

2.5.1 Experimental setup

As in Experiment 2, an horizontal RGB LED strip was attached to a semi-circular structure on the right-hand side of the target (see Figure 3). All LEDs were seen with the same solid angle of 5×10^{-6} sr.

The variations of the LED eccentricity $\theta_S(t)$ was obtained by switching consecutive LEDs on and off along the horizontal trajectory. Seventeen LEDs were used to simulate a moving LED between 5° and 15° eccentricity. Implementing a LED strip to simulate the eccentricity variation eased the design of the experimental device.

The luminance value of the seventeen LEDs were deduced from vertical illuminance (with a LMT B520 luxmeter) measured at seven settings of intensity. For each LED, the relation is linear with a strong correlation ($R^2 > 0.999$). As the solid angle of LEDs was constant, the LEDs luminance values were expected to be close to each other for all intensity settings. The relative standard deviation $\frac{\sigma}{M}$ across the 17 LEDs was about 2.5 %, which shows a small dispersion. Consequently, we have considered the luminance of all LEDs as nearly constant across eccentricities. The luminance range was computed from the average luminance of the 17 LEDs; the extrema are provided in Table 2.

A 5600-K LED lamp was used to generate a background luminance close to 1 cd/m^2 . The luminance value was measured with a Konica Minolta CA-2000 videophotometer (see Table 2).

2.5.2 Experimental protocol

The participants followed the same protocol described in Section 2.3.2, except for the values of L_{ini} and $L_{step,ini}$ (see Table 2). The experiment lasted around 30 minutes.

2.5.3 Experimental design

The four conditions of the experiment (one static and three dynamics) are described in Table 3, and were presented in random order to all participants. Moreover, the static condition ($\theta_S = 10^\circ$, $\omega_S = 5 \times 10^{-6}$ *sr*) was repeated two more times. One of these two repetitions was presented with the eye-tracker on, the other with the eye-tracker off. These additional conditions were carried out either before or after the main experiment. These repetitions allowed checking whether the eye-tracker system impacts the discomfort experienced by the participants. All in all, six staircases were adjusted by the participants during the test session of this experiment.

For each trial of a dynamic staircase, the LED was initially located at $\theta_{max} = 15^\circ$, then the eccentricity decreased down to $\theta_{min} = 5^\circ$, and then increased up to 15° . Thus, the temporal modulation index of eccentricity for the dynamic conditions was 0.5 (see Table 3). This cycle was repeated several times (depending on the frequency) until the end of the trial. The initial value of this signal (see Figure 2(c)) was designed in order to allow the dynamic source to cause less discomfort at the beginning of the trial.

2.6 Experiment 4: Impact of the solid angle variations

2.6.1 Experimental setup

A COB LED was set inside a white closed rectangular wooden box, along with a thermal radiator. The light was emitted toward a convergent lens and an optical diffuser. The light went through a white hollow cylinder before exiting through a motorized diaphragm, which aperture was controlled by an electric step-motor driven by a computer. The only way out of the box for the LED light was through this diaphragm. The electric step-motor allowed to change the apparent size of the glare source dynamically (see Figure 4, top).

The center of the COB LED, the lens, the diaphragm and the participant's eyes were aligned (see Figure 4, bottom). The diaphragm aperture diameter could vary between $\varnothing_{min} = 2$ mm and $\varnothing_{max} = 25$ mm. During the experiment, it changed with time in order for the angular size of the source to follow a periodic cycle (see Figure 2(d)). The time-averaged solid angle

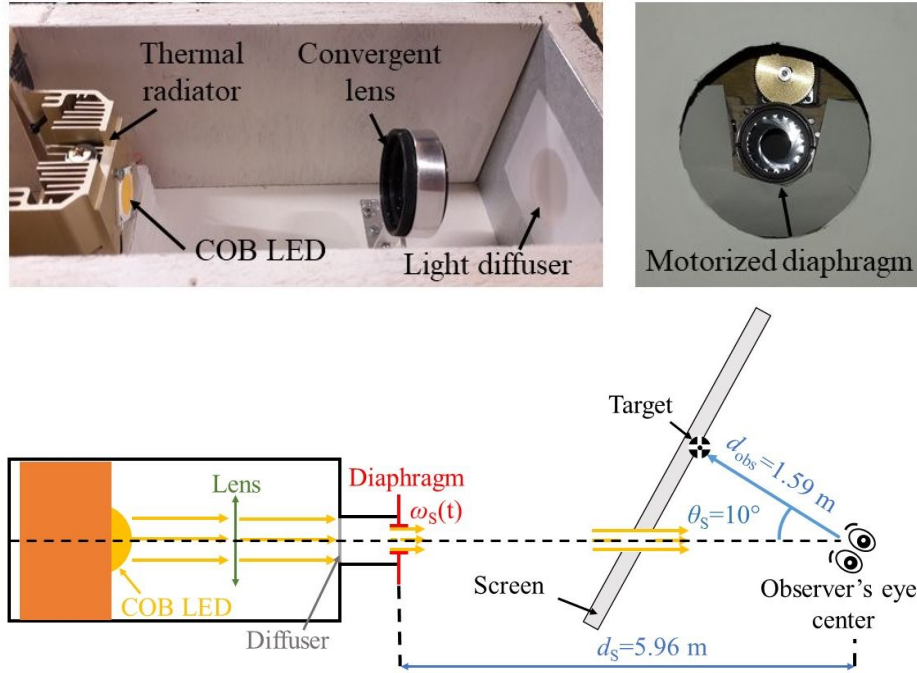


Figure 4: Top Left: The COB LED light source in Experiment 4, together with the thermal radiator, the convergent lens and the optical diffuser. Top Right: the motorized diaphragm. Bottom: Top-view framework of the experimental setup (not to scale).

was $\omega_{av} = 5 \times 10^{-6} \text{ sr}$ in all experimental conditions. This was achieved by choosing the appropriate observation distance, which was set to 5.96 m. With these settings, the solid angle of the source varied between $8.8 \times 10^{-8} \text{ sr}$ and $1.38 \times 10^{-5} \text{ sr}$.

The system was located left to the target, with an eccentricity of 10° . It was behind the screen, where a hole had been cut in order for the source to be entirely visible by both eyes in any conditions (see Figure 4, bottom).

The luminance of the effective luminous surface of the COB LED (delimited by the diaphragm) needed to be constant over time. Two luminance maps of the luminous surface were measured (with a Konica Minolta CA-2000) with the diaphragm diameter at its maximal value: one for the minimal

LED intensity, the other for the maximal intensity. The mean luminance was calculated for five simulated diaphragm diameters, consistent with the periodic signal during the experiment. The mean luminance was 1420 cd/m^2 with the minimum intensity map (with $\frac{\sigma}{M} = 0.62 \%$ across diameters) and 64463 cd/m^2 for the maximum intensity map ($\frac{\sigma}{M} = 0.60 \%$ across diameters). Thus, the mean luminance of the luminous area was considered constant over time, whatever its solid angle.

The background luminance was provided by two 5600-K LED lamps: the first one located behind the participant and oriented towards the screen and the second one located behind the screen and oriented towards the diaphragm. The aim of these two sources was to provide a uniform background luminance close to 1 cd/m^2 both around the target and the glare source. The luminance map of the scene was measured with a Konica Minolta CA-2000 videophotometer: the mean luminance and SD are provided Table 2.

2.6.2 Experimental protocol

The same experimental protocol described in Section 2.3.2 was employed, except for the values of L_{ini} and $L_{step,ini}$ (see Table 2). The whole experiment lasted around 30 minutes.

2.6.3 Experimental design

Four different conditions were presented to the participants in random order (see Table 3): one static ($\theta_S = 10^\circ$, $\omega_S = 5 \times 10^{-6} \text{ sr}$) and three dynamic conditions, with a temporal modulation index equal to 0.99. The static condition was repeated twice: once at the beginning of the experiment for all participants, then randomly. This was intended to compare the two adjustments of the static stimulus, in order to assess the repeatability of the task.

Each dynamic cycle of the LED angular size began with the solid angle minimal value (producing less discomfort), increased until its maximal value (producing more discomfort) and went back to its minimal value (see Figure 2(d)) and so on. The number of cycles depended on the temporal signal frequency.

2.7 Statistical analyses

2.7.1 Dependent Variable

The dependent variable in these experiments was the source luminance at the BCD (L_{BCD}). It was estimated as the average of the luminance in the last four trials of the staircase.

2.7.2 Data rejection criteria

In order to detect and reject potential outliers, two criteria have been considered: one based on the BCD luminance values adjusted by the participants, and one based on the eye-tracker data.

Luminance adjustment The inter-individual variability of glare sensitivity is known to be high. Consequently, some participants would never reach their BCD because of the limited range of source luminance to which they were exposed, given the technical constraints of the experimental devices. The data collected in these situations do not represent the participant's BCD and should therefore be excluded from the analyses.

This is why the data of a participant were rejected from an experiment when the minimum (respectively the maximum) available luminance in a given experiment was reached more than eight times during a staircase, or if the minimum (respectively the maximum) luminance was reached at least twice in a row during the four last trials of a staircase.

Gaze position The participants were instructed to maintain their gaze on the target. In the three experiments where an eye tracker could be used (Experiments 1, 3 and 4), a rejection criterion was established based on visual fixations during the four last trials of each staircase. The distance from the center of the target was computed from the eye-tracker data. If this distance happened to exceed twice the standard deviation of the fixations for more than 5 % of the total duration of the last four trials, the staircase data was rejected. When the data of two staircases were rejected in an experiment, the participant was rejected. If only one staircase was rejected, the missing data was replaced by a weighted average.

2.7.3 Statistical tests

Repeated measures ANOVAs were conducted on the L_{BCD} values in each experiment. Normality was verified with the Shapiro-Wilk test and sphericity with the Mauchly test. When sphericity was not verified, a Greenhouse-Geisser correction was applied. When normality was not verified, a non-parametric Friedman test was applied. The significance level was set to $p = 0.05$. The effect size was estimated with $\eta_{partial}^2$ in ANOVA, the Kendall's W for Friedman test, d of Cohen for t-test, and the correlation coefficient r of Cohen for Wilcoxon signed-rank test.

3 Results

3.1 Preliminary analysis

For each experiment, the number of outlier participants is provided in Table 4. Their data were removed before statistical analyses. In the remaining set, only two data were replaced because of single outlier data (in Experiments 3 and 4).

Table 4: Final panels of each experiment after rejecting the outlier participants.

| Experiment number | Outliers: BCD not reached | Outliers: gaze not onto target | Panel (Women/Men) | Mean Age (SD) |
|-------------------|---------------------------|--------------------------------|-------------------|---------------|
| Exp. 1 | 8 | 2 | 30 (10/20) | 35.8 (12.6) |
| Exp. 2 | 17 | NA | 23 (9/14) | 34.7 (11.6) |
| Exp. 3 | 5 | 0 | 35 (14/21) | 34.3 (11.5) |
| Exp. 4 | 7 | 2 | 31 (13/18) | 31.9 (10.0) |

Mean values of L_{BCD} of the four experiments are provided in Figure 5.

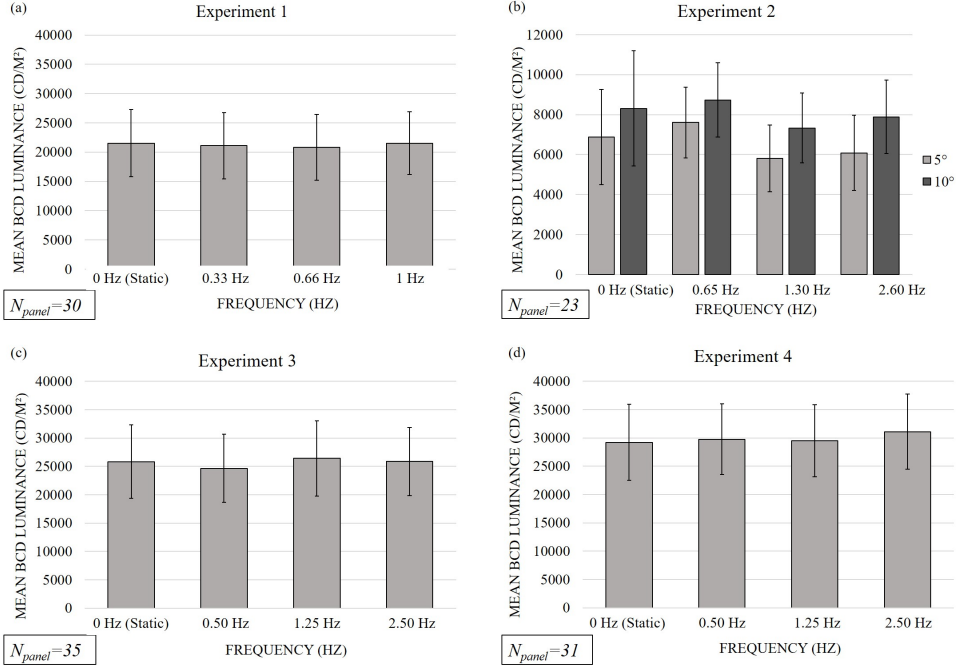


Figure 5: Mean L_{BCD} values in the four experiments: (a) Experiment 1 on the source motion; (b) Experiment 2 on the temporal variations of the source luminance; (c) Experiment 3 on the temporal variations of the source eccentricity; (d) Experiment 4 on the temporal variations of the source solid angle. Error bars shows the 95 % confidence intervals. N_{panel} is the size of the panel in the statistical analysis.

3.2 Experiment 1

Regarding Experiment 1 on the source motion (see Figure 5(a)), the confidence intervals overlap, which suggests that there is no significant difference across conditions between the L_{BCD} values. No significant effect of the frequency of the source motion was found with a repeated measures ANOVA, $F(3,87)=0.312$, $p=0.8169$, $\eta_{partial}^2=0.01063$, Power=10.81 %.

3.3 Experiment 2

Figure 5(b) provides the mean L_{BCD} values for each temporal frequency of the luminance variations, at two eccentricities, with 95% confidence in-

tervals. The mean L_{BCD} value appears higher for 0 Hz and 0.65 Hz than for 1.30 Hz and 2.60 Hz, even though the confidence intervals overlap. As normality was not satisfied, non-parametric Friedman tests were performed independently for each eccentricity. No significant difference was found between the conditions for 5° of eccentricity, $\chi^2(N=23,df=3)=7.032$, $p=0.0709$, $W=0.102$, $r=0.061$, but a significant difference was found for $\theta_S = 10^\circ$, $\chi^2(N=23,df=3)=8.000$, $p = 0.046 < 0.05$, $W=0.116$, $r=0.0758$. Nemenyi post-hoc tests were carried out, and no significant differences were found between any pairs of conditions. Whatever the eccentricity, the Kendall's W is around 0.1 corresponding to a small effect size (Howell, 2009).

A non-parametric test was also conducted with all the data for each factor. A significant difference between the two eccentricities was expected and was found with a large effect with a Wilcoxon signed-rank test, $T=905$, $z=4.81$, $p < 0.001$, $r=0.5$, Power=86.7 %. A significant difference between the four frequencies was also revealed with a Friedman test, $\chi^2(N=46,df=3)=13.85$, $p = 0.0031$, $W=0.1004$, $r=0.0804$. Nemenyi post-hoc tests were carried out and there were significant differences between $f = 0.65$ Hz and the other frequencies ($p = 0.014$ with $f = 0$ Hz; $p = 0.013$ with $f = 1.3$ Hz and $p = 0.029$ with $f = 2.6$ Hz). There were no significant differences between any other frequencies.

3.4 Experiment 3

Figure 5(c) shows that the mean L_{BCD} values are close to each other, and that all confidence intervals overlap. No significant effect of the frequency was found with a repeated measures ANOVA, $F(3,102)=0.632$, $p=0.5959$, $\eta^2_{partial}=0.01825$, Power=17.83 %.

3.5 Experiment 4

Figure 5(d) suggests that the mean L_{BCD} values are close to each other whatever the frequency: all 95 % confidence intervals overlap. The repeated-measures ANOVA did not yield any significant effect of the frequency, $F(3,90)=0.784$, $p=0.5061$, $\eta^2_{partial}=0.0255$, Power=21.3 %.

3.6 Additional analyses

The static condition was repeated twice in experiments 2, 3 and 4 (with one random repetition). These repetitions of the static condition serve as control data and allow to check two methodological issues:

- the intra-individual variability of the panel in Experiments 2, 3 and 4;
- the potential impact of the visible red light from the eye-tracker system in Experiment 3.

3.6.1 Intra-individual variability

Figure 6 shows the mean BCD luminance for the two repetitions of the static conditions in Experiments 2, 3 and 4. In each experiment, the L_{BCD} mean values are very close, with overlapping 95 % confidence intervals. A non parametric Wilcoxon signed-rank test did not reveal any significant difference between the two paired sample data of Experiment 2⁴, $T=263$, $z=-0.322$, $p = 0.75$, $r=0.06$, Power=19 %; and Experiment 4⁵, $T=195$, $z=-0.487$, $p = 0.63$, $r=0.09$, Power=10 %. No significant difference was found either with a t-test in Experiment 3⁶, $t=0.486$, $p = 0.631$, $d=0.028$, Power=7%. It means that the participants reached (on average) the same BCD luminance in the two static conditions, in each experiment, showing a good repeatability of the data.

3.6.2 Eye-tracking

The SMI eye-tracker used in Experiments 1, 3 and 4 emits a low level of visible red light, in addition to infrared light. The vertical illuminance at the observer's eyes due to this red light was not negligible compared to the one due to the glare source. In order to assess whether the eye-tracker impacted the discomfort from glare, the static condition was presented twice in Experiment 3: once with and once without the eye-tracker (see Section 2.5.3). A t-test found no significant difference between the two paired data samples,

⁴The panel was composed of 34 participants (14 women and 20 men), between 20 and 63 years old ($M=35.1 / \sigma=12.3$).

⁵The panel was composed of 31 participants (13 women and 18 men), between 21 and 57 years old ($M=33.4 / \sigma=10.3$).

⁶The panel was composed of 33 participants (15 women and 18 men), between 21 and 57 years old ($M=33.7 / \sigma = 10.5$).

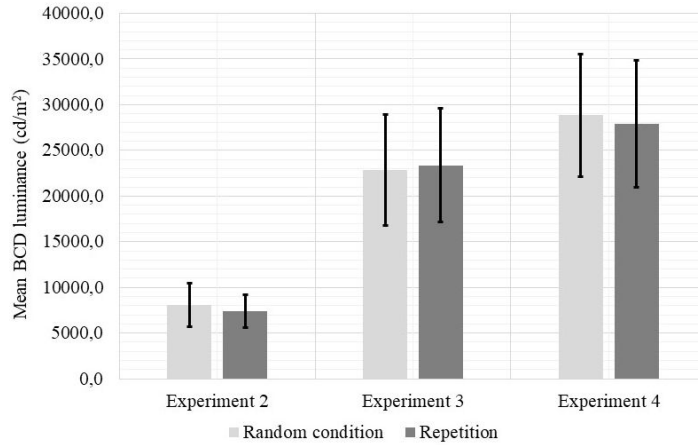


Figure 6: Mean values of the luminance at the BCD for the two repetitions of the static condition (10° , 5×10^{-6} sr) in Experiments 2 ($N_{panel} = 34$), 3 ($N_{panel} = 33$) and 4 ($N_{panel} = 31$). Error bars correspond to the 95 % confidence intervals.

$t=0.676$, $p = 0.504$, $d=0.032$, Power=7%⁷. Thus, the eye-tracker did not impact the participants' settings in the static conditions. We can reasonably extend this result to the dynamic conditions, and to Experiments 1 and 4, where the same eye-tracker was used and where the task was the same.

4 Discussion

Four experiments were independently carried out in order to compare the discomfort from glare in static and dynamic conditions. In each experiment, a single factor of the glare source varied periodically at temporal frequencies representative of outdoor lighting.

4.1 Findings

No significant effect of the frequency was found for:

⁷For this study, seven outliers have been rejected. The final panel was composed of 33 participants (15 women and 18 men), between 21 and 57 years old ($M=33.7 / \sigma = 10.5$).

- $\theta_S(t)$ and $\omega_S(t)$ for $f \leq 2.5$ Hz, with temporal modulation indexes respectively equal to 0.50 and 0.99 (see Sections 3.4 and 3.5);
- $L_S(t)$ for $1.3 \leq f \leq 2.6$ Hz with a temporal modulation index $m = 0.65$ (see Sections 3.3).
- When L_S , θ_S and ω_S are constants, no significant effect of a periodical motion was found for $f \leq 1$ Hz (see Section 3.2).

In Experiment 2, a significant effect of the frequency was found on the discomfort from glare in one case. A dynamic source with $\theta_S = 10^\circ$ and a periodically varying luminance at 0.65 Hz seems to produce less discomfort than a static source, and than the same source at higher frequencies.

The results of Experiment 2 extend the findings of Irikura et al. (1998) towards frequencies lower than 1 Hz, representative of road lighting installations. In their study, the dependent variable was the ratio of the luminance at the BCD adjusted in a dynamic condition (with a temporal frequency between 1 and 16 Hz) and the luminance at the BCD in the corresponding static condition. They tested different background luminances between 0.1 and 100 cd/m^2 ; their results for $L_b = 1 cd/m^2$ can be compared to our data: they found a ratio of 0.80 at 1 Hz and of 0.75 at 2 Hz, meaning that the dynamic condition produced more discomfort than the static one. Contrary to them, we found only one significant difference between a static and a dynamic source in all our experiments.

Considering all four experiments, and except one condition mentioned above (in Experiment 2), no significant difference was found between the static and dynamic conditions in each experiment, in terms of the mean BCD luminance. The dynamic sources were found equivalent (in terms of discomfort from glare) to a static source, in a range of magnitudes relevant for outdoor lighting. These static sources were scaled in such a way that their main characteristics corresponds to the temporal average of the respective periodical signal (mean value of $L_S(t)$ in Experiment 2, mean value of $\theta_S(t)$ in Experiment 3 and mean value of $\omega_S(t)$ in Experiment 4).

For practical applications, it may be useful to extend these findings and neglect the effect of a 0.65 Hz luminance variation for $\theta_S = 10^\circ$ and $m = 0.65$:

this effect shows less discomfort in the dynamic than in the static condition. Thus, it can be proposed to state, as a general rule, that a dynamic source is equivalent to a static source which main factors are the time-averaged values of the dynamic source factors. The exception mentioned above would lead to an over-estimation of the discomfort from glare, which is not critical in the lighting design step.

4.2 Methodological issues

The staircase procedure is prone to the same context effects as usual adjustment tasks (e.g. range effect, etc.) to reach the absolute threshold (Lulla and Bennett, 1981; Poulton, 1989; Fotios et al., 2008). In our experiments, we did not try to estimate these absolute thresholds. We compared static and dynamic conditions with the same context effects (e.g. the same stimulus range, initial value, etc). Thus, the absence of significant difference in our results cannot be due to these context effects.

The technical constraints led to different values of the mean BCD, which can be due to the differences in the glare source spectrum, and to the differences in the available range of stimulus intensities, across experiments. For instance, the luminance range available for the settings was narrower in Experiment 2 than in Experiments 3 and 4 (see Table 2), which may explain why the mean BCD luminance value in the same static condition was below 10000 cd/m^2 in Experiment 2 and above 20000 cd/m^2 in Experiments 3 and 4 (see Figure 6). In Experiment 4, the spectrum of the COB LED has a lower relative energy density in the short wavelengths than the RGB LED used in the other three experiments. As the source spectrum is known to impact the discomfort from glare (Bullough et al., 2003; Sivak et al., 2005; Niedling et al., 2015), a higher mean BCD luminance value was expected compared to the three other experiments (see Figure 6).

Again, we were not interested, in this paper, neither in the absolute values of the luminance at the BCD, nor in the absolute discomfort levels. We only compared, in each of the four independent experiments, the luminance at the BCD in the static and dynamic conditions, and we did not compare the results of the four experiments. Our hypothesis is that any general effect (such as the range effect, or the spectrum effect) would affect similarly

the BCD luminance in both the static and dynamic conditions in a given experiment. Reproducing these experiments with different anchoring points (initial luminance) and different luminance range, as well as others experimental protocols (e.g. ratings scales) would strengthen our findings.

4.3 Limits and perspectives

A large number of outliers have been detected in Experiment 2: many participants did not succeed in reaching the BCD, probably because of the limited luminance range available and the difficulty of adjusting a factor which temporally varied. It would be interesting to reproduce this experiment by adjusting another factor to reach the BCD while the luminance is periodically varying (for instance, adjusting the source eccentricity as in Kim and Kim (2010)).

No eye-tracker system was used in Experiment 2 on the luminance variations. Consequently we were not able to reject participants because of their potential fixations off the target. The low number of outliers detected with this criterion (at most, two participants were rejected in the other experiments, see Table 4) suggests that a large majority of participants have focused their gaze on the target all along the experiments. Thus we can reasonably assume that the absence of eye-tracking system in Experiment 2 only marginally impacts our data.

In Experiment 3, the variation of the LED eccentricity was simulated by switching on and off a series of successive LEDs along a strip, in order to simplify the experimental device. However, the simulated motion was not continuous as in real public lighting conditions. Thus, additional work is needed to confirm our findings by reproducing the same experimental protocol with a continuous motion.

In the four experiments, the periodic variations of the experimental factor were done with a constant value of the temporal modulation index. Even if no significant effect of the frequency was found on the discomfort from glare, it would be interesting to examine how this temporal modulation index impacts the discomfort. Additional work may be conducted, reproducing the experiments of this paper with various temporal modulation indexes.

In our analyses, the statistical power is often weak (lower than 50 %). Even if our tests are less powerful, our effect-sizes are always small (Kendall’s W are around 0.1, and $\eta_{partial}^2$ is close to 0.02). This suggests that if there is an effect of the factor’s frequency on the discomfort from glare (a small effect that our study was not sensitive enough to measure), it is small compared to the main factors usually considered (source luminance, eccentricity and solid angle). Other experiments with larger panels (leading to higher statistical power) may be conducted to assess our findings.

The current work suggests that a dynamic source with one varying factor ($L_S(t)$, $\theta_S(t)$ or $\omega_S(t)$) at the BCD can be considered equivalent (in terms of discomfort) to a static source, where the dynamic factor is replaced by the temporal mean of the dynamic factor. As there is no interaction between the source factors in static situations, it is reasonable to suppose that such a simplification is possible when the three factors vary altogether, as in outdoor scenarios.

Finally, only one background luminance was considered in these experiments ($L_b = 1 \text{ cd/m}^2$). To allow practitioners assessing the discomfort from glare in outdoor environments, the next step will be the development and validation of a model addressing more general situations: other levels of discomfort and background luminance.

5 Conclusion

The impact on the discomfort glare of cyclic variations of the luminance, and of the position and the size of a light source was investigated in four independent psychophysical experiments:

- According to computer simulations, the frequency of the temporal variation of the characteristics of the sources is less than 1 Hz under most public lighting installations and up to 3 Hz in automotive lighting scenarios.
- Up to 1 Hz, no impact of a semi-circular periodic motion of the source was found on the discomfort glare, if its luminance, solid angle and eccentricity are kept constant.

- Up to 2.6 Hz, no impact of the temporal frequency of the glare source's main factors was found, except for a source with variable luminance at a low temporal frequency ($f = 0.65$ Hz) and 10° eccentricity;
- A dynamic source can be considered equivalent to a static source, which main factors are the time-averaged values of the respective dynamic source factors.

Acknowledgments

The authors would like to thank the technical team for its help in the development of the experimental devices, and all the participants who took part in the experiments.

Disclosure statement

No potential conflict of interest was reported by the authors.

Funding

The authors report no funding.

References

- AFE. Recommandations relatives à l'éclairage des voies publiques. Technical report, Association Française de l'Eclairage, Paris, 2002.
- I. Ahmed and C. A. Bennett. Discomfort glare: Duration-intensity relationship. *Journal of the Illuminating Engineering Society*, 8(1):36–39, 1978.
- B. N. Anantha. Discomfort glare: Fry's dynamic disk roadway lighting simulator. Master's thesis, Kansas State University, 1982.
- ANSES. Effects on human health and the environment (fauna and flora) of systems using light-emitting diodes (LEDs). Technical Report 2014-SA-0253, ANSES, Paris, 2019.

- G. Bargary, Y. Jia, and J. L. Barbur. Mechanisms for discomfort glare in central vision. *Investigative ophthalmology & visual science*, 56(1):464–471, 2015.
- C. A. Bennett. Discomfort glare: concentrated sources—parametric study of angularly small sources. *Journal of the Illuminating Engineering Society*, 7(1):2–15, 1977.
- C. A. Bennett. Characterizing discomfort glare from roadway lighting. *Transportation Research Record*, 1149:8–10, 1987.
- J. Bullough and K. Sweater-Hickcox. Interactions among light source luminance, illuminance and size on discomfort glare. *SAE International journal of passenger cars-mechanical systems*, 5:199–202, 2012.
- J. Bullough, J. Van Derlofske, C. R. Fay, and P. Dee. Discomfort glare from headlamps: interactions among spectrum, control of gaze and background light level. In *SAE Technical Paper*, 2003.
- J. Bullough, J. Brons, R. Qi, and M. Rea. Predicting discomfort glare from outdoor lighting installations. *Lighting Research & Technology*, 40(3):225–242, 2008.
- CEN. *EN 13201-2 European Standard: Road Lighting Part 2: Performance requirements*. European Committee for Standardization, Brussels, Belgium, 2015.
- CIE. Glare and uniformity in road lighting installations. Technical Report 31, Commission Internationale de l’Éclairage, Vienna, 1976.
- CIE. Performance assessment method for vehicle headlighting systems. Technical Report 188, Commission Internationale de l’Éclairage, Vienna, 2010.
- CIE. Review of lighting quality measures for interior lighting with LED lighting systems. Technical Report 205, Commission Internationale de l’Éclairage, Vienna, 2013.
- CIE. Discomfort glare in road lighting and vehicle lighting. Technical Report 243, Commission Internationale de l’Éclairage, Vienna, 2021.
- T. N. Cornsweet. The staircase-method in psychophysics. *The American Journal of Psychology*, 75(3):485–491, 1962.

- J. de Boer and D. Schreuder. Glare as a criterion for quality in street lighting. *Transactions of the Illuminating Engineering Society*, 32(2):117–135, 1967.
- DOT. Code de la route, article r412-12, 2003. https://www.legifrance.gouv.fr/codes/article_lc/LEGIARTI000006842131, Ministère des Transports (French DOT).
- DOT. Arrêté du 21 décembre 2005 fixant la liste des affections médicales incompatibles avec l’obtention ou le maintien du permis de conduire ou pouvant donner lieu à la délivrance de permis de conduire de durée de validité limitée : Annexes, 2005. https://www.legifrance.gouv.fr/loda/article_lc/LEGIARTI000022817769/2010-09-15/, Ministère des Transports (French DOT).
- G. Easwer. Discomfort glare: an improved dynamic roadway lighting simulation. Master’s thesis, Kansas State University, 1983.
- M. L. Eble-Hankins and C. E. Waters. VCP and UGR glare evaluation systems: a look back and a look forward. *Leukos*, 1(2):7–38, 2004.
- S. Fotios, K. Houser, and C. Cheal. Counterbalancing needed to avoid bias in side-by-side brightness matching tasks. *Leukos*, 4(4):207–223, 2008.
- K. V. Ganesh. Discomfort glare: variation of light intensity. Master’s thesis, Kansas State University, 1986.
- J. Girard, C. Villa, and R. Brémond. Discomfort glare from several sources: A formula for outdoor lighting. *Leukos*, 8(1):1–17, 2019.
- R. Hopkinson. Discomfort glare in lighted streets. *Transactions of the Illuminating Engineering Society*, 5(1-9):1–32, 1940.
- D. C. Howell. *Statistical methods for psychology*. Cengage Learning, 2009.
- S. A. Hussain. Comparison of real-world roadway lighting, dynamic simulation and cbe and glaremark predictive systems. Master’s thesis, Kansas State University, 1985.
- T. Irikura, Y. Toyofuku, and Y. Aoki. Borderline between comfort and discomfort of blinking light. *Journal of Light & Visual Environment*, 22(2): 12–15, 1998.

- W. Kim and J. T. Kim. A distribution chart of glare sensation over the whole visual field. *Building and Environment*, 45(4):922–928, 2010.
- J. Lee, Y. Choi, X. Yang, G. Oh, M. Kim, H. Kim, J. Kang, and H. You. The effect of visual attention factors on visual field testing for maintenance of gaze fixation. In *Proceedings of the Human Factors and Ergonomics Society Annual Meeting*, volume 61, pages 701–704. SAGE Publications: Los Angeles, CA, 2017.
- P. Lehnert. Disability and discomfort glare under dynamic conditions - the effect of glare stimuli on the human vision. *Progress in Automobile Lighting: Proceedings of the symposium*, 9:582–592, 2001.
- Y. Lin, Y. Liu, Y. Sun, X. Zhu, J. Lai, and I. Heynderickx. Model predicting discomfort glare caused by LED road lights. *Optics Express*, 22(15):18056–18071, 2014.
- Y. Lin, S. Fotios, M. Wei, Y. Liu, W. Guo, and Y. Sun. Eye movement and pupil size constriction under discomfort glare. *Investigative ophthalmology & visual science*, 56(3):1649–1656, 2015.
- T. Liu and S. A. Konz. Simulator studies of discomfort glare in comparison with the CBE prediction. In *Proceedings of the First International Symposium on Glare*, pages 137–142. New York: Lighting Research Institute, 1991.
- M. Luckiesh and S. K. Guth. Brightness in visual field at borderline between comfort and discomfort (BCD). *Journal of Illuminating Engineering*, 44(1):650–670, 1949.
- A. B. Lulla and C. A. Bennett. Discomfort glare: range effects. *Journal of the Illuminating Engineering Society*, 10(2):74–80, 1981.
- M. Niedling, D. Kierdorf, and S. Völker. Influence of a glare sources spectrum on discomfort and disability glare under mesopic conditions. *Lichttechnik*, 4:119–128, 2015.
- E. C. Poulton. *Biais in quantifying judgements*. Taylor & Francis, 1989.
- R. Putnam and W. Gillmore. Discomfort glare at low adaptation levels II-off-axis sources. *Journal of Illuminating Engineering*, 52(4):226–232, 1957.

- H.-J. Schmidt-Clausen and J. T. H. Bindels. Assessment of discomfort glare in motor vehicle lighting. *Lighting Research & Technology*, 6(2):79–88, 1974.
- M. Sivak and P. L. Olson. Toward the development of a field methodology for evaluating discomfort glare from automobile headlamps. *Journal of Safety Research*, 19(3):135–143, 1988.
- M. Sivak, M. J. Flannagan, E. C. Traube, and S. Kojima. The influence of stimulus duration on discomfort glare for persons with and without visual correction. *Transportation Human Factors*, 1(2):147–158, 1997.
- M. Sivak, B. Schoettle, T. Minoda, and M. J. Flannagan. Blue content of LED headlamps and discomfort glare. Technical Report UMTRI-2005-2, University of Michigan, Ann Arbor, Transportation Research Institute, 2005.
- J. M. Stringham and D. M. Snodderly. Enhancing performance while avoiding damage : a contribution of macular pigment. *Investigative Ophthalmology & Visual Science*, 54:6298–6306, 2004.
- L. Thaler, A. C. Schütz, M. A. Goodale, and K. R. Gegenfurtner. What is the best fixation target? the effect of target shape on stability of fixational eye movements. *Vision Research*, 76(1):31–42, 2013.
- W. van Bommel. Visual comfort for motorists. In *Road Lighting*, pages 49–58. Springer, 2015.
- C. E. Waters, R. G. Mistrick, and C. A. Bernecker. Discomfort glare from sources of non-uniform luminance. *Journal of the Illuminating Engineering Society*, 24:73–85, 1995.